PHYSICAL REVIEW B VOLUME 43, NUMBER 4 1 FEBRUARY 1991

Neutron-scattering study of the magnon energies and intensities in iron

M. Yethiraj, R. A. Robinson, and D. S. Sivia
Manuel J. Lujan, Jr. Neutron Scattering Center, Los Alamos National Laboratory, Los Alamos, New Mexico 87545

J. W. Lynn
Department of Physics, University of Maryland, College Park, Maryland 20742

H. A. Mook
Solid State Division, Oak Ridge National Laboratory, Oak Ridge, Tennessee 37831
(Received 23 July 1990)

The magnetic inelastic neutron scattering at low temperatures has been measured from a large single crystal of ^{54}Fe(12 at.% Si) up to energy transfers of 100 meV using the constant-**Q** spectrometer at the Los Alamos pulsed neutron source. The spin-wave energies and intensities were obtained from the data by using a multichannel maximum-entropy technique, and we show that much more detailed information can be obtained from the maximum-entropy analysis. The observed spin-wave dispersion relations obtained in the present experiment are in excellent agreement with earlier data, and we observe a sharp falloff of the (001) magnon intensity at approximately 80 meV, which is in accord with previous experimental measurements and multiband theoretical calculations of the dynamic susceptibility of iron. We also compare the data rate obtained with the constant-**Q** spectrometer to a triple-axis instrument and find that the spectrometer is competitive for this type of measurement.

INTRODUCTION

The spin dynamics of itinerant ferromagnets like Fe, Co, and Ni have been the subject of intense study for many years; partly because they are elemental systems with only one atom in the primitive unit cell and thus they should be the simplest itinerant electron systems to understand theoretically, and partly because iron and its compounds have since ancient times been prototypes for magnetism. Historically, however, the itinerant nature of the 3*d* electrons has not always been obvious. The values of the magnetic moments are nonintegral, which is characteristic of a band ferromagnet, but the susceptibility obeys a Curie-Weiss law, the low-energy spin-wave dispersion relations follow the quadratic form ($E = Dq^2$) expected for a (localized) Heisenberg ferromagnet, and the observed critical phenomena are typical of a conventional three-dimensional ferromagnet. It has only been in recent years that an itinerant description of the 3*d* "magnetic" electrons has become generally accepted as essential, due primarily to results from inelastic neutron scattering,[1] Fermi surface studies,[2] and angle-resolved photoemission measurements.[3]

The most direct method of observing the itinerant character of the "magnetic" electrons is to measure the dynamic susceptibility $\chi(q,\omega)$ via the inelastic scattering of neutrons. This is because the nature of the magnetic excitation spectrum should be qualitatively different depending on whether the spins are itinerant or localized. For a localized spin system the ground-state spin dynamics are characterized by sharp spin waves throughout the Brillouin zone, while for an itinerant system the lifetimes of the spin waves may become quite large in certain regions of the Brillouin zone, making the spin waves appear to vanish. In a single band model, for example,[4] the spin waves would be well defined until the dispersion relation enters the region of the single-particle spin-flip (Stoner) continuum, whereupon their linewidths become comparable to the bandwidth. The magnetic scattering will then be spread over a huge range in energy, and a negligible intensity would be observed within the resolution width of a typical neutron measurement, making the magnons "disappear." In a multiband model, on the other hand, qualitatively new behavior can occur. Numerical calculations of the dynamic susceptibility based on realistic band structures were carried out by Cooke, Lynn, and Davis[5] for both Fe and Ni. The calculations provided a good description of the low energy spin-wave dispersion relations and intensities, while additional "optical" spin-wave modes were predicted to exist at high energies, which were experimentally inaccessible at the time. Blackman, Morgan, and Cooke[6] have recently extended these results by including off-diagonal matrix elements in the calculation of $\chi(q,\omega)$, and these results have in fact been used as a guide in recent neutron experiments. There are certainly still some discrepancies between theory and experiment, but the overall agreement is satisfactory, and can be expected to improve further as more powerful computers become available.

Experimentally, the first measurements reporting itinerant electron behavior using neutron scattering were performed on a triple-axis spectrometer at Oak Ridge National Laboratory by Mook and Nicklow.[7] These are very difficult experiments to carry out at a conventional

thermal neutron source, and they used a large single crystal of ^{54}Fe(4 at. % Si) to improve the signal-to-noise ratio. This isotope of iron was used to reduce unwanted nuclear scattering. The addition of silicon was necessary to permit the growth of a large crystal; its presence does not qualitatively affect the spin dynamics. They observed a rapid drop in the strength of the spin-wave scattering for energies above $\sim$80 meV in all three symmetry directions. After these initial experiments, the isotope crystal was regrown in order to increase its size and mosaic quality. This new sample, presently weighing 166 g, has considerably more Si incorporated in the crystal: 12 at. %. Measurements on this sample by Lynn[8] at Oak Ridge showed that the increased Si content reduces the spin-wave energies by approximately 20% in comparison to pure iron, but the spin-wave intensities still fall-off at high energies.

Measurements of high-energy magnetic excitations are generally very difficult to make with neutrons, because of low neutron fluxes at high energies and the rapid decrease of the magnetic form factor at large wave vectors which necessitates scattering at small angles. In particular, there are a number of significant experimental corrections which must be made to the triple-axis data in order to obtain intensity information over the wide range of energy needed, as discussed elsewhere.[7,8] There has been concern (especially in the early measurements) whether these corrections were made sufficiently well, or whether some unknown instrumental artifact could make the spin wave intensities appear to drop off. More recently, Loong *et al.*[9] carried out measurements on a time-of-flight chopper spectrometer at the Intense Pulsed Neutron Source (IPNS) at the Argonne National Laboratory, where the experimental corrections are of a totally different nature. They observed spin waves in a 23-g crystal of pure iron (with natural isotopic abundance) up to an energy of 160 meV. The measurements were concentrated in the [111] direction, and while these authors did not extract detailed intensity information from their experiment, the observation of spin waves at these high energies appeared to contradict the earlier results which were obtained in the Si doped samples.

In this paper we report measurements on the 166-g sample of ^{54}Fe(12 at. % Si) using the constant-**Q** spectrometer at the Los Alamos pulsed spallation neutron source. This spectrometer employs a pulsed white beam of neutrons incident upon the sample, and then uses the time-of flight technique combined with an analyzer crystal to obtain the spectrum of inelastically scattered neutrons. The instrumental corrections are fundamentally different from those of the triple-axis technique. Our measurements were concentrated close to the [100] crystal symmetry direction. While spin-wave modes are visible in the raw data, we use a novel two-channel maximum entropy (MAXENT) technique to separate the signal from an unknown background and deconvolute the resolution function from the signal simultaneously. This has enabled us to extract the maximum amount of information from the raw data, and allows us to determine the magnon dispersion curve to higher energies and with better intensity sensitivity than is possible from a conventional least-squares analysis of the same raw data. Our results clearly show that the strength of the magnetic scattering decreases, as expected from the earlier triple-axis measurements of Mook and Nicklow[7] and Lynn.[8] We also make some comparisons concerning the utility of the constant-**Q** spectrometer with respect to triple-axis and chopper spectrometers for this type of experiment, and about the general utility of the maximum entropy technique for data analysis.

During the course of this work, Paul *et al.*[10] reported measurements on the same ^{54}Fe(12 at. % Si) sample taken with the IN-1 "hot source" triple-axis spectrometer at the Institut Laue Langevin. In the [100] direction they found that the strength of scattering dropped rapidly above approximately 75 meV and became unobservable, but the spin waves reappeared above approximately 200 meV. In the [111] direction, however, the spin waves were broadened and reduced in intensity at higher energies, but magnetic scattering could be observed all the way to the zone boundary. Hence the apparent contradiction between the original triple-axis experiments[7] and the recent time-of-flight data[9,11] in the pure iron sample appears to be resolved. The overall agreement of both triple-axis and time-of-flight experiments is quite good, and they clearly show the itinerant character of the magnetic electrons.

EXPERIMENTAL METHOD

As stated above, the measurements were performed on a large single crystal of ^{54}Fe (12 at. % Si). The silicon was added to stabilize the sample in the body-centered cubic α phase at all temperatures, though 12 at. % Si is rather more than is strictly necessary. Below 4 at. % Si content, a face-centered-cubic γ phase exists at high temperatures[12] and this severely complicates the crystal growth of single crystals of pure iron. The isotopic sample minimizes both the coherent and incoherent nuclear scattering, since ^{54}Fe has the smallest nuclear scattering length of any Fe isotope and, by coincidence, Si has the same scattering length as ^{54}Fe. This is the identical single crystal that was used by Lynn[8] and by Paul *et al.*[10]

The spectrometer used in this study was the constant-**Q** Spectrometer at LANSCE, the pulsed spallation neutron source at Los Alamos. The spectrometer is shown schematically in Fig. 1. The constant-**Q** geometry was originally proposed by Windsor *et al.*,[13] who built a prototype at Harwell. The idea behind the spectrometer geometry is to be able to measure a complete constant-**Q** scan for each setting of the spectrometer and sample crystal. To do this, the analyzer is set such that the component of **Q** perpendicular to the incident beam, $Q_\perp$, is kept constant and the spectrometer takes data in the $Q_\parallel, E$ plane, where $Q_\parallel$ is the component of **Q** parallel to the incident wave vector. A concise and general description of the kinematics for constant-$Q_\perp$ spectrometers has been given by Robinson and Pynn.[14] The present spectrometer, which is fully described elsewhere,[15,16] follows Windsor's concept but includes many improvements. In particular, for this experiment, we used a large multicomponent copper analyzer.[17] This particular analyzer

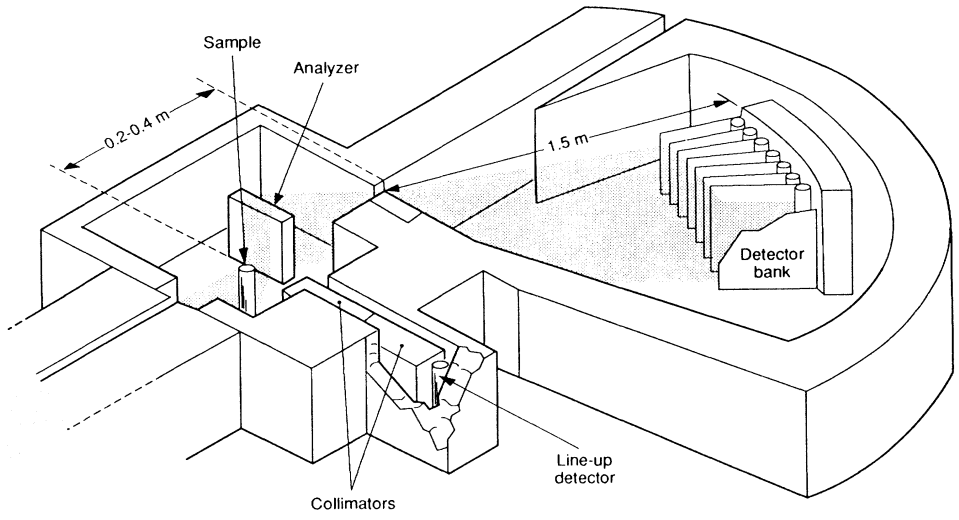

FIG. 1. A schematic view of the Los Alamos constant-**Q** spectrometer. Neutrons arrive from the left and strike a single crystal sample. The scattered neutrons are energy analyzed by a large crystal analyzer and detector array.

configuration, the "organ-pipe" configuration,[15,17] allows one to use any of the reflections in the $\langle hhk \rangle$ zone. In this study, we have used the (002) and (111) analyzer reflections.

Measurements were made at both room temperature and 10 K. In the latter case, cooling was provided by a closed-cycle Displex refrigerator. Some penalty was incurred in the low-energy background due to the scattering from the aluminum-alloy cryostat tails, but in the energy regime of interest, the background was reduced on cooling.

The sample was aligned with the [001] axis vertical. All measurements were made with the spectrometer locus running directly through either the (110) or the (200) reciprocal lattice points in Fe. This means that one should see two spin-wave branches spaced symmetrically about the $Q_{\parallel}$ corresponding to the reciprocal lattice point. The range in $(Q_{\parallel}E)$ that can be accessed is limited to a plane determined by the analyzer d spacing. In our case, these geometrical considerations restricted us to take data 11° away from the [010] direction rather than along the symmetry direction. In Fig. 2(a), $Q_{\perp}$ is fixed by the choice of

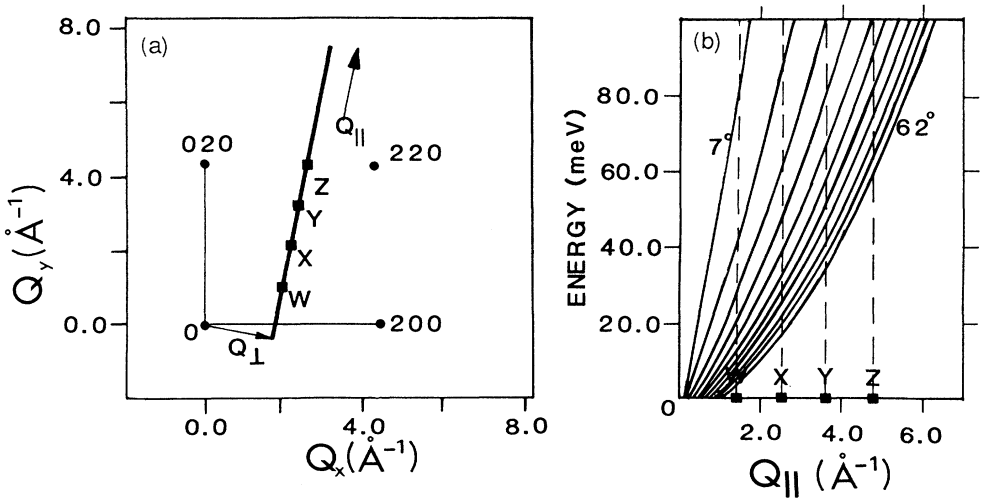

FIG. 2. (a) The scan direction for the data discussed in the text and (b) the lines are detector loci starting for the first detector at 7° and ending with the last detector at 62°. (Only every tenth detector locus is plotted.) The area in between is the accessible range in $(Q_{\parallel}E)$.

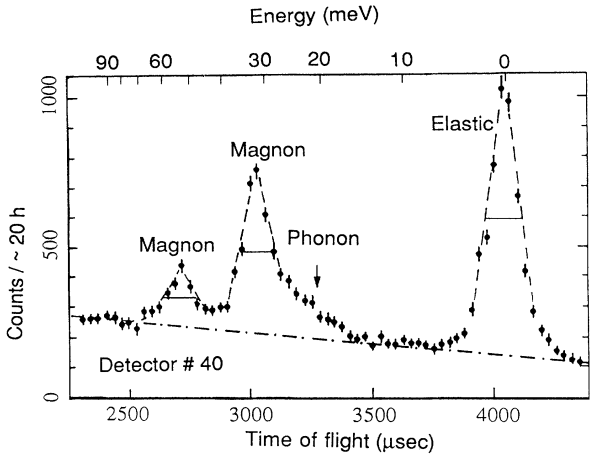

FIG. 3. A typical detector spectrum in time of flight, from which it can be seen that the signal is much sharper than the background and that the background can be approximated by a straight line. Note that the peaks all have roughly the same width in time of flight.

the Cu(002) analyzer and the measurements are made for **Q** values in a line perpendicular to $Q_\perp$. Further, the range in energy varies with $Q_\parallel$. The shaded region in Fig. 2(b) shows the total $(Q_\parallel, E)$ area accessible for the chosen scan through the (110) reciprocal lattice point in Fe using the Cu (002) analyzer. This data set was taken with the sample cooled to 10 K and is the configuration in which our best data were obtained, particularly with respect to the energy transfer range covered. A time-of-flight spectrum from a single detector is shown in Fig. 3.

DATA ANALYSIS—MAXIMUM ENTROPY

The problem of reducing our data is that a large quantity of data is collected as a function of scattering angle ϕ and time of flight t. In these coordinates, the instrumental corrections are relatively straightforward and the resolution does not vary strongly. However, the physics of interest is best thought of in wave vector and energy transfer space, **Q** and E. The transformations[14] between these coordinate systems are straightforward but nonlinear. At some point in the analysis, one must perform a two-dimensional nonlinear rebinning from (ϕ, t) to $(Q_\parallel E)$ and make all appropriate corrections to the intensities.[15] The problem with doing this on the raw data is that statistical fluctuations are propagated in a correlated way into a number of bins in the $Q_\parallel E$ space. Furthermore, in these coordinates, the resolution changes greatly. It is clearly better to perform any smoothing or deconvolution, and correct for ϕ-dependent systematic effects like the background, in the ϕ, t space and then rebin into $Q_\parallel$ and E. The maximum entropy method is the best way to do this.

We have chosen to deconvolute our data using the maximum entropy method. However, because the instrumental resolution is not sufficiently well known, we do not perform a "strict deconvolution." It has been shown[18] that the resolution function need not be known with absolute accuracy to obtain reasonable estimates of the positions and relative intensities of peaks. In general, utilizing a width slightly greater than the real resolution results in suppressing ringing artifacts.

The maximum entropy (MAXENT) technique is a general image reconstruction method which is routine in a wide variety of fields, including ratio astronomy, photographic enhancement, and medical imaging. More recently, this method has been applied to a number of different types of problems in neutron-scattering data analysis.[19]

We describe here the multichannel MAXENT used to analyze our data. Our primary reason for choosing to carry out the data analysis by this method is that it provides a good model-independent way of estimating the scattering law. We do not make any *a priori* assumptions about the number, type, or shape of the excitation dispersion curves inherent in the scattering law. The general properties of the MAXENT technique are as follows. (a) Several statistical arguments strongly suggest that MAXENT is the preferred method for inferring positive additive distributions, such as the neutron-scattering law, (b) MAXENT enforces positivity, and (c) MAXENT tends to put structure in the reconstructed image (inferred scattering law) only if it is warranted by the data. As such, we are using MAXENT as a powerful tool to help with the data analysis, but this technique is not central to our conclusions. Detailed explanations of MAXENT can be found in Refs. 20–23 (and references therein).

We begin by illustrating the use of MAXENT on a simple simulation of a straightforward convolution problem, computed on a grid of 128 points. We start off with a test profile, which we refer to as the "true" object. Our "true" object, shown in Fig. 4(a), consists of two spikes separated by a small plateau on the left and a broader peak on the right. Since we assume that the resolution function of the constant-**Q** spectrometer can be approximated by a Gaussian, we convolved our "true" object with the broad Gaussian shown in Fig. 4(b); we added to this blurred object a small flat background (about 5% of the peak signal) and random $\sqrt{N}$ noise, to generate the simulated data set shown in Fig. 4(c). Given these data, and a knowledge of the background and resolution function, Fig. 4(d) shows the MAXENT reconstruction of the object. This is a very satisfactory reconstruction in that we see no spurious features, and the "true" structure has been recovered with approximately the correct positions and integrated intensities. If the spikes had been much closer together, however, the integrated intensities of the individual peaks would not necessarily have been preserved although the total flux in the reconstruction would be conserved. We also note that the two sharp spikes are reproduced with a finite width rather than as δ functions; this is because there is not enough information in the data (alone) to safely infer the presence of sharper structure.[18,19,24]

Next we consider the more difficult case when, as for our constant-**Q** data, the background function is not known. To deal with this situation we need to use a more

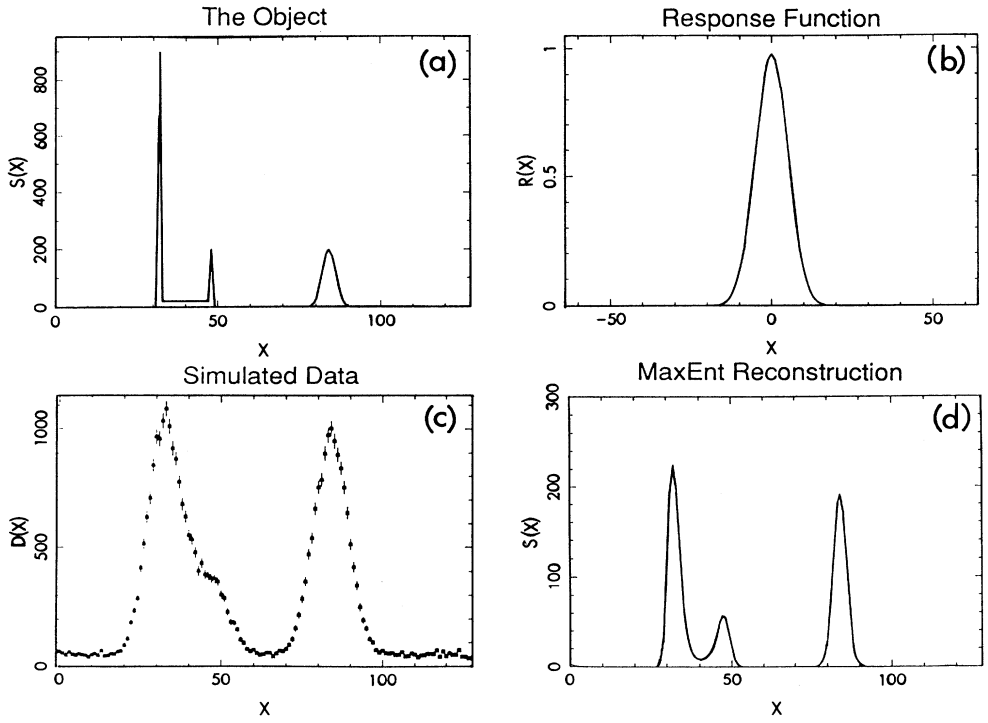

FIG. 4. A simple maximum entropy simulation: (a) the "true" object, (b) the resolution function which is, in this case, a Gaussian, (c) the simulated data, obtained by convoluting the object with the resolution function and then adding a small background and random noise, and (d) the MAXENT reconstruction of the object.

advanced MAXENT technique: multichannel entropy.[25] We can use this method to make an automatic separation between broad structure, which we will interpret as the "unknown background," and sharp structure, which we will interpret as the scattering law of interest. In essence, we create two "image" (or reconstruction) channels with the following properties: (a) one channel is only allowed to have broad structure while the second is permitted high resolution and (b) it is arranged so that it is "entropically cheaper" to put structure in the broad-feature channel rather than in the high-resolution channel. This ensures that if the broad structure can account for the data, it will appear in the broad-feature channel; if sharp structure is required, it can only appear in the high-resolution channel. An algorithm designed to implement this idea is described elsewhere,[19] but we demonstrate its use on another simple simulation.

The set-up is much the same as before. The object in Fig. 4(a) was convolved with the resolution function of Fig. 4(b), but now a large broad background was added to generate the noisy data set shown in Fig. 5(a). These data are far worse than our raw data, but the exaggeration merely serves to emphasize the power of the analysis method. Figure 5(b) and 5(c) are the MAXENT reconstruction for the signal and background channels, respectively, obtained using the algorithm outlined above. This is quite impressive given the data.

For the analysis of our Fe data, the multichannel entropy algorithm of[19] was generalized to two dimensions and the only correction made to the raw data was to divide it by the integrated intensity for an elastic incoherent scatterer (ZrH_2), detector by detector. For the broad-feature channel, we assumed that the background was linear in t for each detector, but the slope and intercept of this line was allowed to vary from detector to detector. The linear assumption appears to be borne out in practice by both the raw data and the ZrH_2 (normalization) scans, and is a more stringent constraint on the nature of the background channel than the "broad-feature" criterion used in Fig. 5. This formulation has the advantage that changes in the background cannot account for data which give rise to sharp features in the scattering law, while it still allows enough flexibility to accommodate different levels of noise in the various detectors.

For computational reasons, the MAXENT reconstruction is carried out in the ϕ-t space since, in this space, an invariant resolution function in (ϕ,t) is a reasonable approximation. We have used the resolution calculation of Ref. 15 to study the variation of the spectrometer resolution function over the range of interest in this experiment. The angular resolution is constant to within better than $\pm 10\%$ over the whole map. The time-of-flight resolution at the elastic line is calculated to be independent of the scattering angle within better than $\pm 10\%$. This is in agreement with the data in Fig. 6. However, the calculated time resolution for energy loss scattering decreases significantly with increasing energy transfer and is small-

er by a factor of 2 (of the elastic value) for energy transfers of 100 meV. For this particular data set, however, the inelastic peaks are as broad as the elastic line as can be seen in Fig. 3. Presumably, this is due to intrinsic broadening of the excitation and we can assume that the resolution is constant in dt and $d\phi$ over the entire map. Even if that were not strictly true, it has been shown[18] that the positional information obtained in this manner will still be reliable. Although relative intensities at the highest energy transfers will be underestimated, this error will be small compared to the dramatic drop in magnetic intensity that is observed. Of course, to extract correct information on the magnon lifetimes, use of the correct spectrometer resolution is imperative and the above approximations should not be made. The transformation to energy, being nonlinear, preserves neither the constant resolution nor the linear background, as can be seen from the energy scale plotted along the top of Fig. 3. For the spectrometer resolution we have assumed an invariant Gaussian resolution function, with a full-width-half-maximum of approximately 150 μs in time and 1.3° in detector angle.

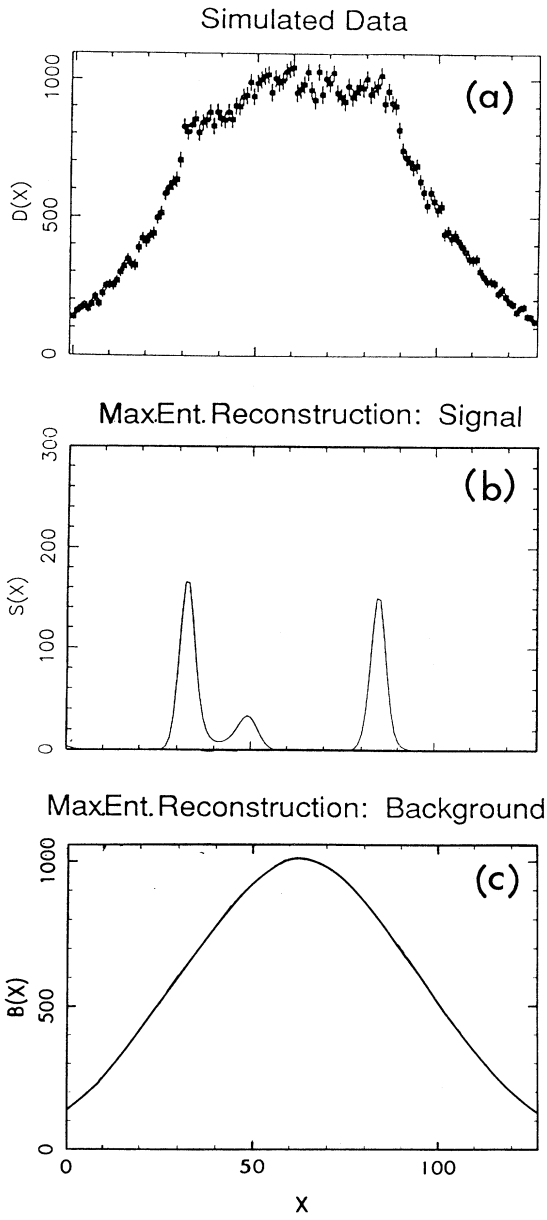

FIG. 5. (a) The simulated data, obtained by convoluting the object [Fig. 4(a)] with the Gaussian resolution function [Fig. 4(b)] and then adding a larger, broad "unknown" background. (b) The MAXENT reconstruction for the signal channel and (c) the reconstructed background channel.

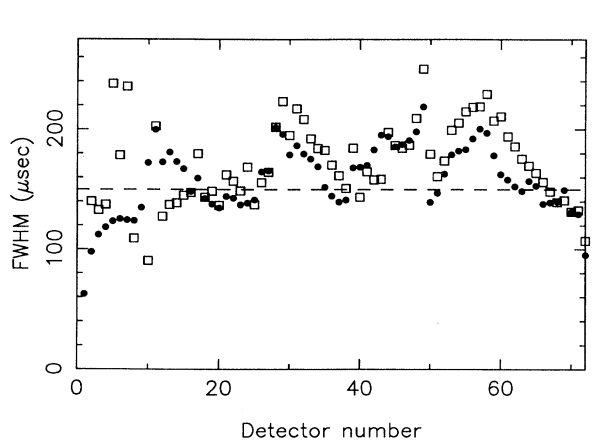

FIG. 6. The elastic widths (FWHM for a Gaussian fit) in time-of-flight as a function of detector angle. The solid circles are for the ZrH_2 normalization scan and the open squares are for the Fe data. The dashed line is the width of the Gaussian resolution function used in the MAXENT reconstruction.

RESULTS

The data for the scan roughly along the [001] direction are shown in Fig. 7(a), as a function of the experimental variables, time-of-flight (t) and detector angle (ϕ). The data suffer from a combination of broadening and an unknown background signal (in addition to $\sqrt{N}$ noise), which obscures the scattering law of interest. Figure 7(b) is the MAXENT reconstruction of the signal (high-resolution) channel, showing a dramatic improvement in both the detail seen in the scattering law and in the reduction of background artifacts.

In Fig. 7(b), the three inelastic features are labeled A,B (which correspond to the $-q$ and $+q$ branches of the magnon, respectively) and C (the transverse phonon excitation) in order of their intensities. Clearly, A and B are much sharper in the reconstruction than in the raw data. This width in time would lead to a larger error in energy and momentum transfer when transformed to these physically relevant units. While this is impressive, perhaps the more dramatic part of the reconstruction is the feature labeled C. The raw data counterpart of C is a

shoulder on the high-t side of the most intense inelastic peak (A); this is now resolved in the reconstruction, especially at lower angles, as can be seen in Fig. 7(b). A one-dimensional plot of a typical detector is shown in Fig. 7(c).

In addition, a broad horizontal feature labeled X is seen in the raw data which disappears in the reconstruction. This intensity can obviously be taken care of by the background channel alone and is due to a few slightly noisy detectors.

The centers of the peaks in the MAXENT signal channel are now transformed to momentum and energy transfer in Fig. 8. The features A, B, and C correspond to the $(-q)$ branch of the magnon, the $(+q)$ branch of the magnon and a phonon that is mainly transverse in character, respectively. In order to compare these results with previous measurements, the quadratic equation $E=dq^2$ (where D is the stiffness constant and set equal to 230 meV Å^2) is plotted as a solid line. The dashed line is the Born-von Kármán calculation for the transverse phonon along this particular direction using force constants from previous work by Brockhouse *et al.*[26] There is also a longitudinal phonon in this vicinity, but its intensity is insignificant for this experimental geometry. The agreement between the present data and the previous work is excellent.

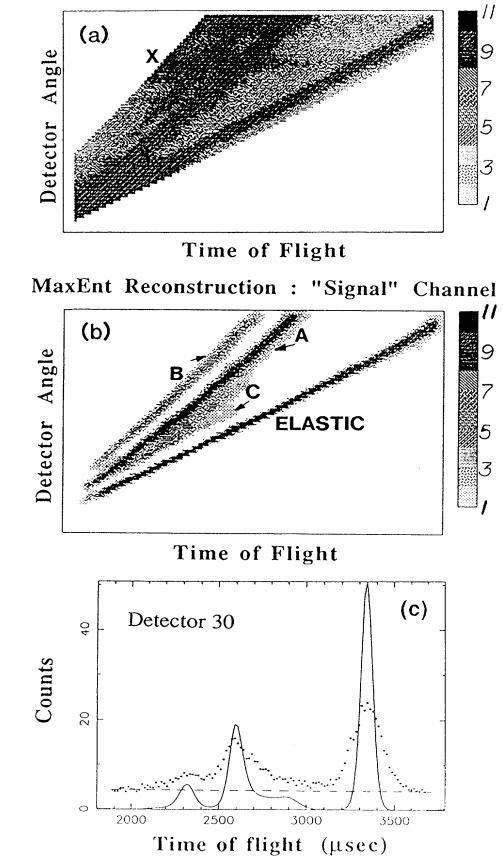

FIG. 7. Maximum entropy treatment of our raw data in ϕ,t space: (a) The raw data and (b) the MAXENT reconstructed high resolution channel. The ϕ and t limits were chosen to include all the data of interest, while the upper left band excludes second-order contamination and the lower right bound excludes energy-gain scattering. A and B refer to the $-q$ and $+q$ magnon branches, respectively, while C refers to a transverse phonon mode.

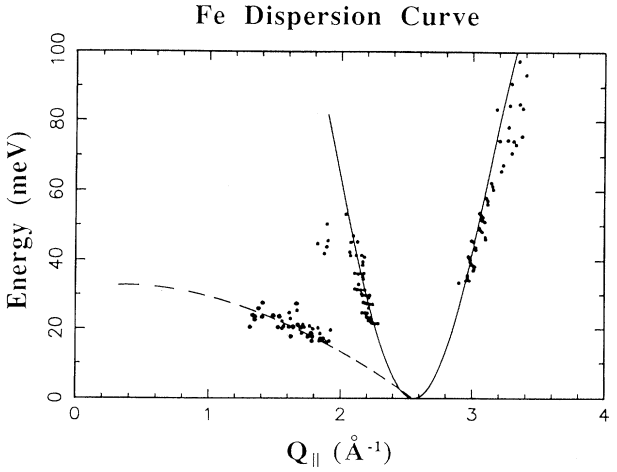

FIG. 8. The dispersion curve obtained by converting the centers of the peaks in the MAXENT high-resolution channel to units of energy and momentum transfer. The solid line is the quadratic $E=Dq^2$, where D, the stiffness constant $=230$ meV Å^2 and the dashed line is the transverse phonon calculated from published force constants (Ref. 26).

The MAXENT technique tends not to put any structure in the reconstruction that is not supported by the data. This leads the reconstruction to be smooth in a statistically significant fashion. The smoothness of the reconstructed image avoids the pitfalls of propagating statistical fluctuations in (ϕ,t) into $Q_{\|}$-E coordinates when performing the two-dimensional nonlinear rebinning, since a single (ϕ,t) pixel can contribute to several $(Q_{\|},E)$ bins, especially at small ϕ.

The entire MAXENT signal channel is now transformed to a $Q_{\|}$-E map, following the transformations given by Robinson and Pynn,[14] and is shown in Fig. 9(a). The intensities were corrected for the effects of variation in incident spectrum and instrumental resolution volume, following the recipe given in the Appendix to Ref. 15. Note that the intensity at high energy has disappeared on the $+q$ side, while there is still significant intensity at the same scattering angle, at lower energies. This is strong evidence for the drop in intensity on the $+q$ side being a real physical effect, rather than an instrumental artifact. The intensity profiles, rather than merely the positions of the three excitations, can be seen more clearly in this map. In comparison, the dispersion relations obtained

from the raw data are shown in Fig. 9(b), and Fig. 9(c) shows the $Q_{\parallel}$-E map obtained when the MAXENT background was subtracted from the raw data prior to the conversion to $Q_{\parallel}$ and E. As one might expect, the raw data without any background subtraction is an extremely poor representation of the dispersion surface. But even using the same (MAXENT) background, the nondeconvolved picture has not resolved the $(-q)$ magnon and phonon excitations into being two distinct features as the MAXENT image has done. In other words, in Fig. 9(c), the $(-q)$ magnon branch and that TA phonon branch run together and cannot easily be separated. In addition, the $(+q)$ magnon branch (B) is clear enough in the MAXENT picture to be transformed to higher than 90 meV. It is important to note that there are no artifacts in the reconstruction.

Since the $(+q)$ magnon branch is well separated from the other peaks, it is expected that the integrated flux in this peak will be conserved locally. However, this is not necessarily true for the $(-q)$ branch of the magnon due to its proximity to the phonon excitation. In this case, the total flux of the two excitations should be conserved, but the individual peak flux may not be. From the $Q_{\parallel}$-E map, the magnon intensities are obtained by integrating over $Q_{\parallel}$ at constant energy. These intensities are corrected for the variation of the magnetic form factor as a function of Q.[27] In the energy range of 40–100 meV, the dispersion curve is linear. Hence, as the angle between the integration direction (constant E) and the dispersion surface is independent of Q, no further corrections are made to the magnon intensity. The integrated magnon intensity as a function of energy is shown in Fig. 10 and agrees well with the data in Ref. 7. The large number of data points in this figure is simply due to the choice of a 64×64 pixel array to represent the (1.5–3.5 Å^{-1}, 0–100 meV) $Q_{\parallel}$-E map. Each pixel in the $Q_{\parallel}$-E map is correlated with its nearest neighbors and will cause the adjacent points in Fig. 10 to have strongly correlated errors. Hence, the local variations of the magnon intensity as a function of energy may not be significant. The present data are represented by the points while the solid curve is the original triple-axis data,[7] which is given for comparison.

At first glance it may seem that a drop in intensity of this magnitude would render the excitation unobservable at 100 meV. However, it must be borne in mind that the Jacobian of the transformation from (ϕ,t) to (Q,E) varies by almost a factor of 20 between 40 and 100 meV. Hence, the observed drop in intensity would be only one order of magnitude. In addition, the normalization by the incoherent scatterer can also account for more than 2 orders of magnitude. Again, since the time resolution was overestimated by a factor of 2 for 100-meV energy

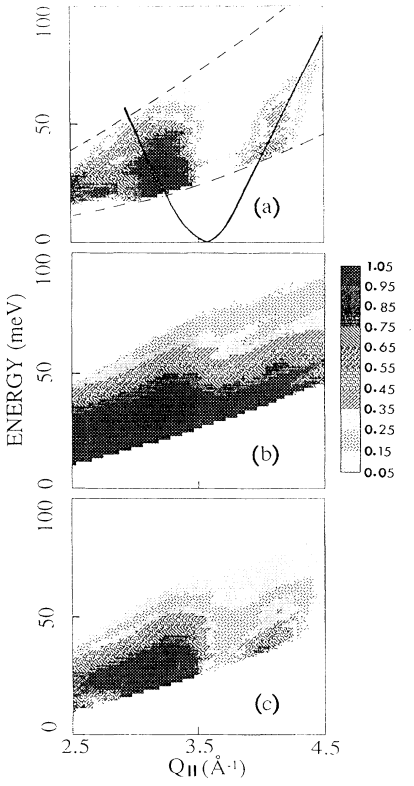

FIG. 9. (a) The entire MAXENT reconstruction from Fig. 7(b) rebinned into $Q_{\parallel}$ and E coordinates, in comparison to (b) the $Q_{\parallel}$-E map of the raw data and (c) the $Q_{\parallel}$-E map of the raw data with the MAXENT background subtracted from the data prior to rebinning into $Q_{\parallel}$ and E. Again, the zone center (i.e., 110 reciprocal lattice point in Fe) corresponds to $Q_{\parallel}=2.56$ Å^{-1}. The solid line is the quadratic $E=Dq^2$, where $D=230$ meV Å^2. The intensity scale is logarithmic and has been truncated to provide the best contrast for the $+q$ spin waves.

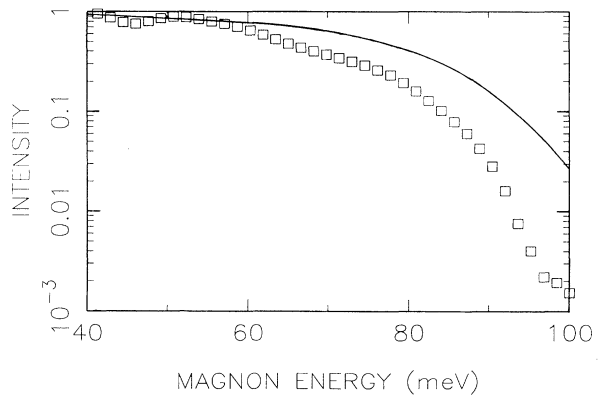

FIG. 10. A plot of spin-wave intensity as a function of energy transfer, corrected for the effects of variation in incident spectrum, instrumental resolution volume, and form factor. The present data are represented by the open squares. The corrected magnon intensity shows a sharp fall-off in the scattering at approximately 80 meV. The solid line which is from Ref. 7, has not been corrected for instrumental resolution.

transfer excitations, the intensity of the 100-meV magnon maybe be underestimated by as much as a factor of 2. It should be noted that the present data have been corrected for instrumental resolution by the MAXENT technique and hence, represent the intrinsic spin-wave intensity. The original triple-axis data, on the other hand, still include instrumental resolution. The effect of the resolution will be to spread out the intensity in energy. This may account for a slower falloff than the intrinsic intensity. Considering that the present data underestimate the intensity and that the original triple-axis data have rather large error bars at higher energies, the overall agreement is reasonable.

DISCUSSION AND CONCLUSIONS

There are three principal results of the present work. The first addresses the physics of itinerant electron magnets. A rapid decrease of the magnon intensity with increasing energy has been observed close to the [001] symmetry direction. The instrumental conditions and corrections in the present case are fundamentally different than for triple-axis spectrometers, and the present data confirm the basic results that have been obtained with the triple-axis technique. The data are consistent with each other, and are in semiquantitative agreement with calculations of the dynamic susceptibility of the band electrons of iron.[5,6]

The second aspect concerns the performance of the constant-Q spectrometer. Considerable spectrometer time was used to set up the experimental and test various instrumental conditions, but the actual data we analyzed and reported here were obtained in a total running time of approximately 20 h, with the proton storage ring delivering ~ 30 μA to the spallation target. Reliable spin wave energies and intensities, as well as a portion of a phonon branch, were obtained over an energy range from ~ 20 to 100 meV. Thus it is clear that the data collection rate is quite high. The background in the present experiment was also rather high, but even so, the signal-to-background ratio (in the raw data) was approximately 1:1.5 in the range of 80–85 meV. In comparison, the measurement of a single magnon peak along the [001] direction at 83 meV energy transfer took over 4 hr, using a traditional triple-axis spectrometer at HFIR at Oak Ridge,[7] where the signal-to-background ratio was approximately 2:1. Furthermore, the background varied strongly and the assumption of linearity may be unjustified. In contrast, our background is almost flat and can be identified on both sides of the scattering of interest.

A number of substantial improvements could be made which would enhance the performance of the instrument. The incident beam collimator only uses approximately 35% of the available moderator field of view,[28] as the present collimator was designed and built at a time when the upstream aperture could be placed no closer than 2.24 m from the moderator. The field of view was reduced substantially in order for the sample to view only the moderator. The moderator size has also been increased since the spectrometer was built. Hence with a new collimator the incident flux onto the sample could be increased by a factor of 3. In addition, the proton beam current incident on the neutron production target during these experiments was approximately 30 μA. Thus a further increase in flux of a factor of 3 can be realized when the PSR, currently operating at 60 μA, achieves its design current of 100 μA. An additional increase in intensity, as well as a reduction in background, could also be obtained by using Be analyzers instead of Cu. It would also be worthwhile to install a "t_0" chopper to block the beam at the time (t_0) that protons strike the target and thereby reduce the background due to unwanted fast neutrons. If the above improvements were carried out, it would then be possible for the magnon branch in Fe to be measured up to 100 meV in under 2 hr, which would be considered an impressive achievement even in the most conservative circles.

Finally we turn to a discussion of the maximum entropy data analysis technique, and to a comparison of the method of carrying out experiments on the spectrometer versus a conventional triple-axis instrument. The constant-Q spectrometer, as any time-of-flight instrument, maps out large regions of $(\mathbf{Q},E)$ space simultaneously. Under favorable conditions, the region where the data are collected is of direct interest, and a large amount of usable data can be collected at the same time. Often, however, in setting up to observe a particular dispersion surface, much of the $(\mathbf{Q},E)$ space where data are collected may not contain any signal and hence these data will be of no use. In addition, geometrical restrictions caused us to take data along a direction in reciprocal space which was 11° from the [010] direction, rather than exactly along the symmetry direction as would be preferred. With a triple-axis spectrometer on the other hand, we can in principle make measurements at any chosen $(\mathbf{Q},E)$, and thus can measure along any of the principal symmetry directions, or at off-symmetry points, at the experimenters' discretion. These measurements are rather time consuming, though, and generally data are taken only in narrow "known" regions of interest. Thus it is less likely that a totally unexpected result would be obtained with the triple-axis technique.

The simplicity of the triple-axis data usually makes the data analysis straightforward. Typically the instrumental resolution does not vary significantly over the range of a scan, and then a least-squares fit of a measured peak with a Gaussian or Lorentzian is sufficient to extract the essential information such as the position, width, and intensity of the excitation. With the vast amount of data obtained with the time-of-flight technique, on the other we need a data analysis procedure which can extract the maximum amount of information from the data, in a systematic and unprejudiced way. The maximum entropy method is clearly the method of choice for this purpose. It assures the positivity of the cross section, and extracts the best estimate of the intrinsic cross section from the data in a statistically significant way, but without making any assumptions about the number of excitations or detailed shape of the scattering function (such as a Gaussian or Lorentzian).

One of the powerful features of the MAXENT technique

is that we can include in a systematic way "prior knowledge" of what the scattering cross section should be. One obvious requirement which must always be valid is that the cross section be positive definite, and the MAXENT technique incorporates this in a natural way. In our present analysis, though, we have made an additional assumption that the scattering can be separated into two components—one channel contains only a relatively broad feature whereas the other we assume consists of distinctly sharper peaks. This is additional "prior knowledge" that we are putting into the analysis, since we "expect" sharp magnon and phonon peaks, and an instrumental background which is very broad. The two-channel analysis in fact does an impressive job of analyzing the data in this way, and of extracting the signal from the "background." The detailed energies and intensities of the magnons which have been obtained from the present data (Figs. 8 and 10) could not have been extracted at the higher energies by a traditional least-squares fitting method. This was also the case for the data obtained earlier at IPNS.[9] It is important to keep in mind, however, that the two-channel analysis is strictly an assumption and as such must be checked for consistency at the end of the analysis. In fact in the present case the magnetic intensity, integrated over all energies (up to the bandwidth), should be a constant, and the intensity which is disappearing from the sharp magnon peak should be distributed over a very large energy range which is expected to be too large to have an observable signal over the range of energies explored here. With the present analysis technique, though, any broad magnetic component would be included with the "background" channel, and hence would not be properly identified. At elevated temperatures, in addition, where the magnetic scattering is known to be broad, the two-channel technique might not be very successful in properly identifying the magnetic scattering.

In conclusion, we have confirmed the itinerant electron behavior of magnetism in iron and have demonstrated that, even with a first-generation instrument, spallation sources are competitive with reactors in terms of intensity for this type of experiment. It is clear that maximum entropy techniques should become an essential and routine part of data collection and analysis procedures in the field of neutron scattering.

ACKNOWLEDGMENTS

Research at Los Alamos was supported, in part, by the division of Basic Energy Sciences of the U.S. Department of Energy. Research at Maryland was supported by the NSF Grant DMR89-21878. Research at Oak Ridge was supported by the Division of Materials Sciences, U.S. Department of Energy under contract DC-AC05-84 OR21400 with Martin Marietta Energy Systems.

[1]See, for example, H. A. Mook, in *Spin Waves and Magnetic Excitations,* edited by A. S. Borovik-Romanov and S. K. Sinha (North-Holland, Amsterdam, 1988), Chap. 7.

[2]G. G. Lonzarich, in *Electrons at the Fermi Surface,* edited by M. Springford (Cambridge University Press, Cambridge, England, 1980), pp. 225–277.

[3]A. M. Turner, A. W. Donoho, and J. L. Erskine, Phys. Rev. B **29**, 2986 (1984).

[4]E. D. Thompson, Phys. Rev. Lett. **19**, 635 (1967).

[5]J. F. Cooke, J. W. Lynn, and H. L. Davis, Solid State Commun. **20**, 799 (1976); Phys. Rev. B **21**, 4118 (1980).

[6]J. A. Blackman, T. Morgan, and J. F. Cooke, Phys. Rev. Lett. **55**, 2814 (1985).

[7]H. A. Mook and R. M. Nicklow, Phys. Rev. B **7**, 336 (1973).

[8]J. W. Lynn, Phys. Rev. B **11**, 2624 (1975).

[9]C.-K. Loong, J. M. Carpenter, J. W. Lynn, R. A. Robinson, and H. A. Mook, J. Appl. Phys. **55**, 1895 (1984).

[10]D. McK. Paul, P. W. Mitchell, H. A. Mook, and U. Steigenberger, Phys. Rev. B **38**, 580 (1988).

[11]Paul *et al.* (Ref. 10) incorrectly assumed that the time-of-flight scans made by Loong *et al.* (Ref. 5) somehow averaged over q. Figure 1 of Ref. 9 shows that their constant-E scans were typically within 11° of the [111] direction. The fact that relatively well-defined spin waves were observed up to 160 meV seems to be fortuitous coincidence of the symmetry direction for which data were obtained.

[12]M. Hansen, *Constitution of Binary Alloys* (McGraw-Hill, New York, 1958).

[13]C. G. Windsor, R. K. Heenan, B. C. Boland, and D. F. R. Mildner, Nucl. Instrum. Methods **151**, 477 (1978).

[14]R. A. Robinson and R. Pynn, Nucl. Instrum. Methods **A272**, 758 (1988).

[15]R. A. Robinson, R. Pynn, and J. Eckert, Nucl. Instrum. Methods **A241**, 312 (1985).

[16]M. Yethiraj and R. A. Robinson, in *Advanced Neutron Sources 1988,* Inst. of Physics Conf. Ser. **97**, 395 (1989).

[17]M. Yethiraj and R. A. Robinson, in *Advanced Neutron Sources 1988,* Inst. of Physics Conf. Ser. **97**, 389 (1989).

[18]D. S. Sivia, R. N. Silver, and R. Pynn, Nucl. Instrum. Methods **A287**, 538 (1990).

[19]R. N. Silver, D. S. Sivia, and R. Pynn, in *Advanced Neutron Sources 1988,* Inst. of Physics Conf. Ser. **97**, 673 (1989).

[20]E. T. Jaynes, *Papers on Probability, Statistics and Statistical Physics, Collected Works, (1957–1980),* edited by R. D. Rosenkrantz (Reidel, Boston, 1983; reprinted, Kluwer Academic, Boson, 1989).

[21]S. F. Gull, and J. Skilling, IEE Proc. **131F**, 646 (1984).

[22]J. Skilling and R. K. Bryan, Mon. Not. R. Astron. Soc. **211**, 111 (1984).

[23]J. Skilling and S. F. Gull, in *Maximum Entropy and Bayesian Methods, Cambridge, 1988,* edited by J. Skilling (Kluwer Academic, Boston, 1989).

[24]D. S. Sivia, in *Maximum Entropy and Bayesian Methods, Dartmouth, 1989,* edited by P. Fougere (Kluwer Academic, Boston, 1990), pp. 195-209.

[25]T. J. Newton, Ph.D. thesis, Cambridge University, 1985.

[26]B. N. Brockhouse, H. E. Abou-Helal, and E. D. Hallman, Solid State Commun. **5**, 211 (1967).

[27]C. G. Shull and Y. Yamada, J. Phys. Soc. Jpn. **17**, Suppl. B **111**, 1 (1962).

[28]J. S. Gilmore, R. A. Robinson and G. J. Russell, in *Advanced Neutron Sources 1988,* Inst. of Physics Conf. Ser. **97**, 469 (1989).